



# Stresses in Prosthetic Elbow Joint During Flexion-Extension Movement

Daniela Tarnita<sup>1</sup>(✉) , Dragos Popa<sup>1</sup> , Cristian Boborelu<sup>2</sup>, Mirela Cherciu<sup>1</sup> ,  
Corina Cernaianu<sup>1</sup> , Laura Grigorie<sup>1</sup> , Alina Romanescu<sup>1</sup> ,  
and Danut-Nicolae Tarnita<sup>2</sup>

<sup>1</sup> University of Craiova, Craiova, Romania  
daniela.tarnita@edu.ucv.ro

<sup>2</sup> Emergency Hospital of Dolj County, Craiova, Romania

**Abstract.** The present paper aims to study the virtual behavior of a prosthetic elbow joint. The values and distribution of stresses in the prosthetic elbow joint by using FEA on the 3D virtual model during flexion-extension movement under the solicitation of a vertical external force are obtained. They are compared with those developed on the human healthy elbow joint. Solid Works software is used in order to obtain the virtual model and Visual Nastran to obtain the von Mises stress by finite element analysis. The maximum stresses values in metallic components of prosthetic elbow are about 4–5 times higher than those obtained in healthy elbow, for a flexion angle equal to 90 degrees.

**Keywords:** Virtual prosthetic elbow · von Mises stress · finite element analysis

## 1 Introduction

The finite element analysis (FEA) applied on virtual models is used more and more in the field of research in orthopedics or traumatology as a modern, efficient and accurate method for studying the behavior of human bones and joints [1–23]. FEA is often used to study the kinematic and dynamic behavior of the human musculoskeletal system, healthy bones, broken and implanted bones [1–4], as well as normal, osteoarthritic or prosthetic joints of lower limbs [5–11] and upper limbs [12–18]. FEA allows researchers to test virtual human bones, joints, bone-implants and joints-implants assemblies in order to study their biomechanical behavior or to design new implants and perform their optimization [2–4, 11, 15, 17]. FEA studies were developed in order to analyze and optimize bioinspired robotic structures, often used in rehabilitation [8, 9, 11, 19–24]. Virtual modeling of the healthy and prosthetic human elbow, simulations and FEA analyses of its biomechanical behavior, as well as the study of stresses occurred in the human elbow joint under various loads were addressed in several articles [12–15, 17, 18].

The aim of this research is to evaluate the values and distribution of stresses in the prosthetic elbow joint by using FEA on the 3D virtual model during flexion-extension movement under the solicitation of a vertical external force and compare them with those developed on the healthy elbow.

## 2 FEA Analysis of the Virtual Model of the Prosthetic Elbow Joint

The Tornier-Latitude prosthesis system is a complex modular implant with great constructive flexibility, offering the possibility, depending on the situation found intraoperatively by surgeons, but also the residual instability, to move, intraoperatively, from an unconstrained prosthesis to one constrained by use of a piece that attaches to the ulnar component. The virtual model of the Tornier-Latitude total elbow prosthesis was developed based on the measurements and commercial prospectus of the product [16] and is presented in detail in the article [18], Fig. 1.

To determine the dynamic stress maps, the complex virtual model of the prosthesis elbow joint was exported to the finite element analysis software. The virtual simulation corresponds to the raising and lowering of a force of 100N, having a permanent vertical action and the application point located at the extremities of the ulna and radius, by the flexion and extension movement, having a total duration  $T = 1$  s. In order to run the analysis with finite elements method, it is necessary to divide all the components of the Latitude prosthesis into finite elements. The main mechanical characteristics of each component of the prosthetic elbow will be provided, as input data.

Figure 2 shows the discretized virtual models for the humeral component and the ulnar component, while their mechanical characteristics are shown in Table 1.

Mesh structure of closing ulnar component, closing bushing, ulnar stem bushing, humeral ax, spherical coupling, radial stem are shown in Fig. 3, while the main mechanical characteristics are presented in Table 2 and Table 3. We noted HDPE – high density polyethylene.

The finite element structures of the radial head, the humeral stem screw, the spherical dome screw and the ulnar stem screw are shown in Fig. 4, and their mechanical characteristics are shown in Table 4.

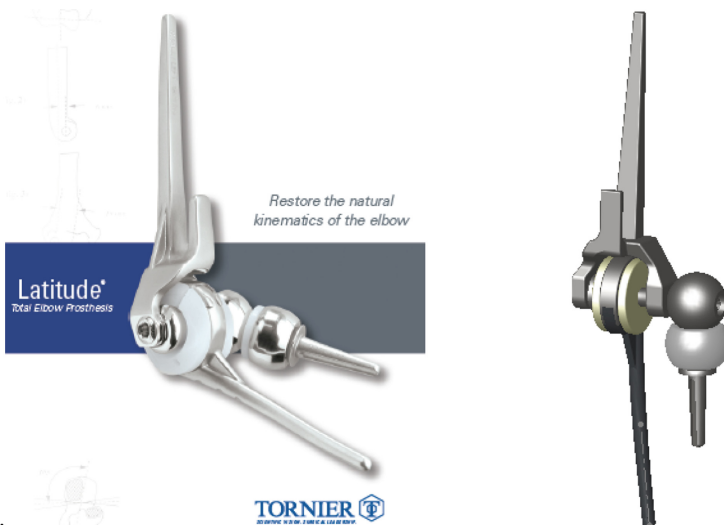


**Fig. 1.** Latitude total elbow prosthesis: a) Prosthetic prospectus [16]; b) the virtual model [18]

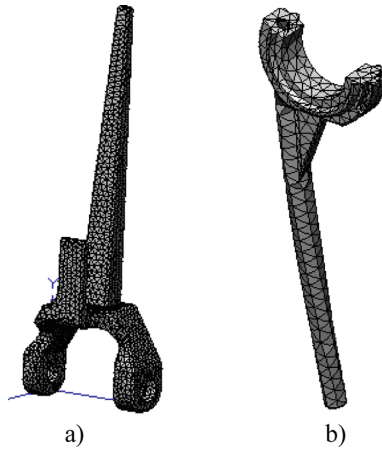


**Fig. 2.** Mesh structure of: a) humeral component; b) ulnar component

**Table 1.** Main mechanical characteristics of humeral component and ulnar component

<b>Component</b>		
<b>Properties</b>	<b>Humeral component</b>	<b>Ulnar component</b>
Material	Titan	Titan
Density $\text{kg}/\text{mm}^3$	4.85e-6	4.85e-6
Masa, (kg)	0.0158 kg	0.00656 kg
Young's module (Pa)	1.02e + 11 Pa	1.02e + 11 Pa
Poisson's ratio	0.3	0.3
Nodes number	26199	5093
Elements number	15676	2783

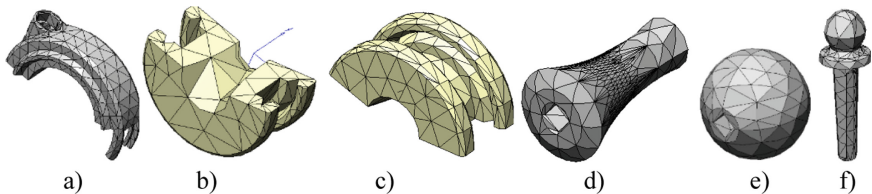


**Fig. 3.** Mesh structure of: a) closing ulnar component, b) closing bushing, c) ulnar stem bushing, d) humeral ax, e) spherical coupling, f) radial stem

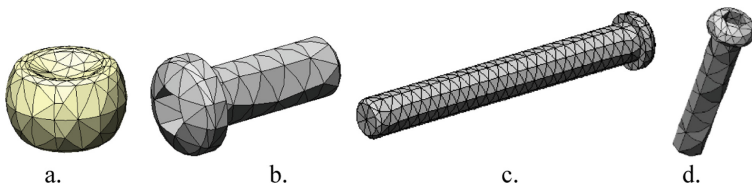
The three human bones: humerus, cubitus and radius, which are components in this assembly, were also divided into finite elements after they were prepared (cut) for virtual arthroplasty (Fig. 5), and their mechanical characteristics are shown in Table 5.

**Table 2.** Main mechanical characteristics of closing ulnar component, closing bushing, ulnar stem bushing

<b>Component</b>			
<b>Properties</b>	<b>Closing ulnar component</b>	<b>Closing bushing</b>	<b>Ulnar stem bushing</b>
Material	Titan	HDPE	HDPE
Density kg/mm <sup>3</sup>	4.85e-6	9.52e-7	9.52e-7
Mass, (kg)	0.00267	0.000933	0.000746
Young's module (GPa)	1.02	1.07	1.07
Poisson's ratio	0.3	0.41	0.41
Nodes number	2974	1180	2338
Elements number	1644	550	1280

**Table 3.** Main mechanical characteristics of humeral ax, spherical coupling, radial stem

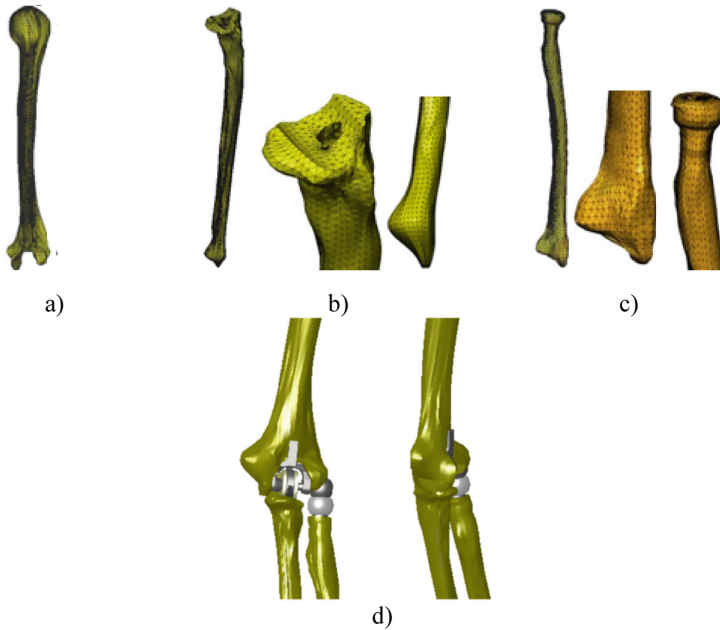
<b>Component</b>			
<b>Properties</b>	<b>Humeral ax</b>	<b>Spherical coupling</b>	<b>Radial stem</b>
Material	Titan	Titan	Titan
Density kg/mm <sup>3</sup>	4.85e-6	4.85e-6	4.85e-6
Mass (kg)	23.6 e-4	92.5e-4	30.4e-4
Young's module (GPa)	114	114	114
Poisson's ratio	0.3	0.3	0.3
Nodes number	4223	1116	1034
Elements number	2404	615	508

**Fig. 4.** Finite elements structure of: a) radial head; b) screw of humeral stem; c) screw of spherical coupling; d) screw of ulnar stem

The complex virtual model of prosthetic elbow joint is composed of 118875 finite elements and 202704 nodes. The humerus was the fixed component, the other elements were considered mobile. In humero-ulnar and humero-radial rotation joints, a driving

**Table 4.** Main mechanical characteristics of radial head, screw of humeral stem, screw of spherical coupling and screw of ulnar stem

<b>Component</b>				
<b>Properties</b>	<b>Radial Head</b>	<b>Screw of humeral stem</b>	<b>Screw of spherical coupling</b>	<b>Screw of ulnar stem</b>
Material	HDPE	Titan	Titan	Titan
Density kg/mm <sup>3</sup>	9.52e-7	4.85e-6	4.85e-6	4.85e-6
Mass (kg)	9.14e-4	3.8e-4	8.8 e-4	1.7 e-4
Young's module (GPa)	1.07	114	114	114
Poisson's ratio	0.41	0.3	0.3	0.3
Nodes number	1383	704	2799	631
Elements number	710	344	1512	300

**Fig. 5.** Mesh structure of: a) humerus, b) cubitus (ulna); c) radius; d) virtual model of prosthetic elbow joint

**Table 5.** Main mechanical characteristics of: humerus, cubitus and radius

<b>Component</b>			
<b>Properties</b>	<b>Humerus</b>	<b>Cubitus</b>	<b>Radius</b>
Material	Cortical bone	Cortical bone	Cortical bone
Density kg/mm <sup>3</sup>	1.4e-5	1.4e-5	1.4e-5
Mass (kg)	2.19	0.431	0.595
Young's module (GPa)	21.4	21.4	21.4
Poisson's ratio	0.5	0.5	0.5
Nodes number	56313	48839	47878
Elements number	33562	28742	28245

movement was defined having an angular velocity  $\dot{\alpha} = -450 \sin(2\pi t)$  deg/s. Figure 6 shows frames of the dynamic stress map for flexion-extension movements.

### 3 Discussions

Based on the stresses maps in Fig. 6, the diagram of the maximum von Mises stresses in the prosthetic elbow joint during flexion-extension movements for the analyzed period was drawn (Fig. 7), and compared to the diagram corresponding to the healthy (non-prosthetic) elbow, obtained and explained in detail in [15].

One conclusion is that the maximum stresses values are recorded in both cases for an angle of 90 degrees between the arm and forearm, when the bending moment is maximum, while minimum stresses are recorded in the maximum flexion position and the maximum extension position when the bending moment is very small, about 0. The maximum stresses values in prosthetic elbow are about 280 MPa, about 4–5 times higher than those obtained in healthy elbow, 75 MPa, but in first case, the maximum stresses are distributed on the prosthesis' components and they remain within admissible material strength values. Even the stresses present an important increase in the maximum tension states in the prosthetic elbow joint, they are developed on the prosthetic components, while the bones are solicited under normal demand. In the case of the prosthesis elbow, the maximum stresses are recorded in the contact area of the radial head prosthesis, which is a stress concentrator caused by the variation of the section.

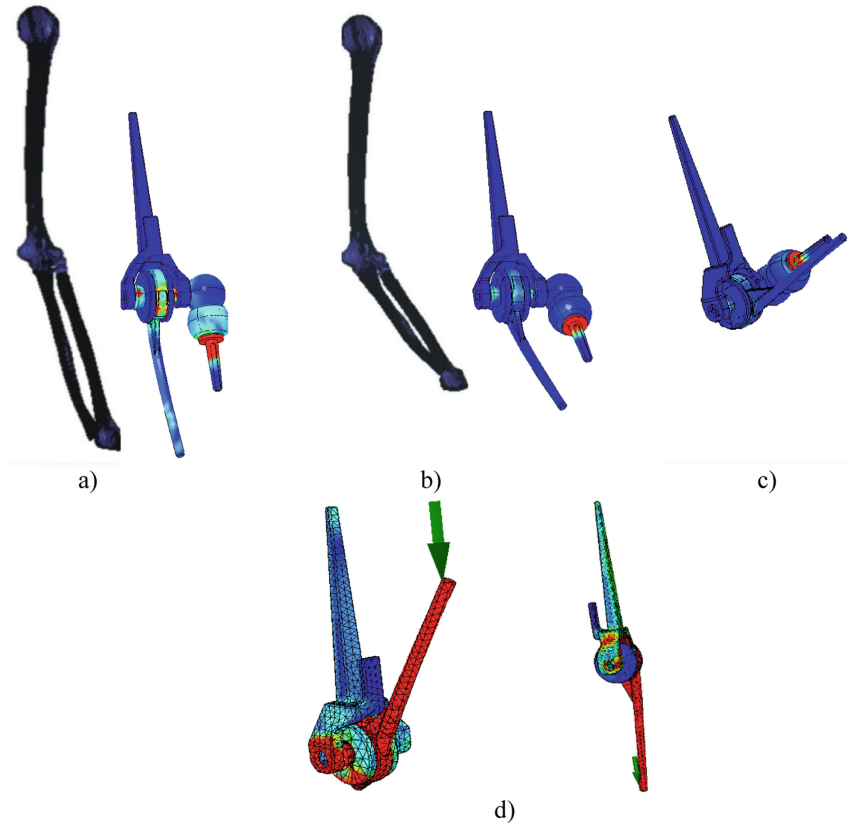


**Fig. 6.** Stress map for prosthetic elbow joint in flexion-extension movement for a)  $t = 0$  s, b)  $t = 0.2$  s, c)  $t = 0.8$  s and d) prosthetic device in total flexion and total extension

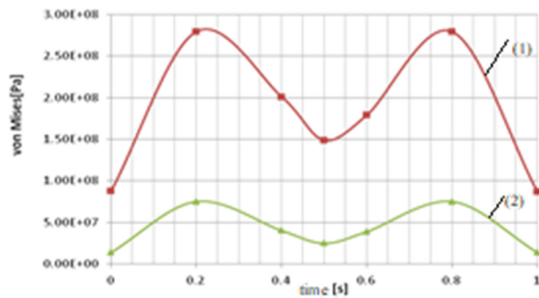


**Fig. 7.** Comparative von Mises stress variation for a cycle of flexion-extension movement of prosthetic elbow (1) and healthy elbow (2)

## 4 Conclusions

This paper presents the results of dynamic simulation of the flexion-extension movement of the Latitude prosthesis-joint assembly. The Latitude (Tornier, Stafford, TX) total elbow system, currently offers to surgeons the options of performing a hemiarthroplasty or a conversion from an unlinked to a linked total elbow arthroplasty, allowing that the later revision can be performed without the need to remove well-fixed stems. Using the Solidworks parameterized modelling environment, numerical simulations and FEM analyses were performed for flexion-extension of the assembly of elbow joint- prosthesis. Based on the developed stresses maps, the comparative diagrams of the maximum von Mises stresses developed during the flexion-extension movements of the healthy elbow and of the prosthetic elbow were drawn.

**Acknowledgment.** This research is supported by the funds of Project 546/2020, code PN-III-P2-2.1-PED-2019-3022, “Innovative modular robotic system for medical recovery of brachial monoparesis-NeuroAssist” funded by UEFISCDI.

## References

1. Taddei, F., Cristofolini, L., et al.: Subject-specific finite element models of long bones: An in vitro evaluation of the overall accuracy. *J Biomechanics* 39(13), 2457–2467 (2006).
2. Tarnita, D., et al.: Numerical simulations of human tibia osteosynthesis using modular plates based on Nitinol staples. *Rom J Morphol Embryol* 51(1), 145-150 (2010).
3. Tarnita, D., et al.: In vitro experiment of the modular orthopedic plate based on Niti used for human radius bone fractures. *Rom. J. Morphol Embryol* 51(2), 315–320 (2010).
4. Tarnita, D., Tarnita, D.N., Bizdoaca, N., et al.: Modular adaptive bone plate for humerus bone osteosynthesis. *Rom. J. Morphol Embryol* 50(3), 447–452 (2009).
5. Lee H.Y., Kim S.J., et al.: The effect of tibial posterior slope on contact force and ligaments stresses in posterior-stabilized total knee arthroplasty-explicit finite element analysis. *Knee Surg Relat Res* 24(2), 91–98 (2012).
6. Tarnita, D., Catana, M., Tarnita, DN.: Contributions on the modeling and simulation of the human knee joint with applications to the robotic structures, In *Mechanisms and Machine Science* vol. 20, pp. 283-297. Springer Verlag (2014).
7. Tarnita, D., et al: Contributions on the dynamic simulation of the virtual model of the human knee joint, *Materials Science and Engineering Technology* 40(1-2), 73-81 (2009).
8. Tarniță, D., Tarniță, D.N., Bizdoaca, N., Boborelu, C., et al.: Modular adaptive bone plate for humerus bone osteosynthesis. *Rom J Morphol Embryol* 50(3), 447-452 (2009).
9. Tarnita, D., Catana, M., et al.: Design and Simulation of an Orthotic Device for Patients with Osteoarthritis, In Bleuler, H., et al. (eds) *New Trends in Medical and Service Robots. Mechanisms and Machine Science*, vol 38, pp. 61–77. Springer, Cham (2016).
10. Villa, T., et al.: Contact stresses and fatigue life in a knee prosthesis: comparison between in vitro measurement and computational simulations. *J. Biomechanics* 37, 45-53 (2004).
11. Tarnita, D., et al.: Orthopedic implants based on shape memory alloys. In: Fazel R (ed) *Biomedical Engineering–From Theory to Applications* 18, pp. 431-468. InTech, Viena (2011).
12. Lan, N., Murakata, T.: A realistic human elbow model for dynamic simulation. *Moment* 3(4), 5 (2001).



13. Tarnita, D., Boborelu, C., Popa, D., Rusu, L.: The three-dimensional modeling of the complex virtual human elbow joint. *Rom. J. Morphol Embryol* 51(3), 489–495 (2010).
14. Zhang, L. et al.: Upper limb musculo-skeletal model for biomechanical investigation of elbow flexion movement. *Journal of Shanghai Jiaotong Univ. (Science)* 16(1), 61–64 (2011).
15. Tarnita, D. et al.: Design and Finite Element Analysis of a New Spherical Prosthesis-Elbow Assembly. *Mech. and Machine Science* 57, pp. 127-135, Springer, (2018).
16. <https://www.wright.com/products-upper/latitude-ev-total-shoulder-arthroplasty>
17. de Vos MJ, et al.: Short-term clinical results of revision elbow arthroplasty using the latitude total elbow arthroplasty. *The Bone Joint Journal* 98-B(8),1086–92 (2016).
18. Tarnita, D., et al.: Virtual Modeling and Numerical Simulations of the Latitude Prosthesis-Human Elbow Assembly. In: Dumitru I., et al (eds) *The 30th SIAR Intern. Congress of Automotive and Transport Eng., SMAT 2019*, pp.706-712, Springer (2020).
19. Geonea, I., Tarnita, D.: Design and evaluation of a new exoskeleton for gait rehabilitation. *Mechanical Sciences* 8(2), 307-322 (2017).
20. Tarnita, D., Pisla, D., Geonea, I., Vaida, C., I. et al.: Static and Dynamic Analysis of Osteoarthritic and Orthotic Human Knee. *J Bionic Eng.* 16, 514-525 (2019).
21. Geonea, I., et al.: Dynamic Analysis of a Spherical Parallel Robot Used for Brachial Monoparesis Rehabilitation. *Appl. Sci.* 11, 11849 (2021). <https://doi.org/10.3390/app112411849>.
22. Pisla, D. et al.: A Parallel Robot with Torque Monitoring for Brachial Monoparesis Rehabilitation Tasks. *Appl. Sci.* 11, 9932 (2021). <https://doi.org/10.3390/app11219932>.
23. Tarnita, D., Berceanu, C., et al.: The three-dimensional printing—a modern technology used for biomedical prototypes. *Materiale Plastice* 47(3), 328–334 (2010).
24. Dumitru, N., et al.: Dynamic Analysis of an Exoskeleton New Ankle Joint Mechanism. In *New Trends in Mechanism and Machine Science*, vol. 24, pp 709-717, Springer (2015).

**Open Access** This chapter is licensed under the terms of the Creative Commons Attribution-NonCommercial 4.0 International License (<http://creativecommons.org/licenses/by-nc/4.0/>), which permits any noncommercial use, sharing, adaptation, distribution and reproduction in any medium or format, as long as you give appropriate credit to the original author(s) and the source, provide a link to the Creative Commons license and indicate if changes were made.

The images or other third party material in this chapter are included in the chapter's Creative Commons license, unless indicated otherwise in a credit line to the material. If material is not included in the chapter's Creative Commons license and your intended use is not permitted by statutory regulation or exceeds the permitted use, you will need to obtain permission directly from the copyright holder.

